Title	TEMPERATURE FIELD AND ITS EFFECTS ON A LONG-SPAN STEEL CABLE-STAYED BRIDGE BASED ON MONITORING DATA
Author(s)	ZHOU, YI; SUN, LIMIN; SUN, SHOUWANG
Citation	Proceedings of the Thirteenth East Asia-Pacific Conference on Structural Engineering and Construction (EASEC-13), September 11-13, 2013, Sapporo, Japan, A-2-1., A-2-1
Issue Date	2013-09-11
Doc URL	http://hdl.handle.net/2115/54204
Type	proceedings
Note	The Thirteenth East Asia-Pacific Conference on Structural Engineering and Construction (EASEC-13), September 11-13, 2013, Sapporo, Japan.
File Information	easec13-A-2-1.pdf

Instructions for use

TEMPERATURE FIELD AND ITS EFFECTS ON A LONG-SPAN STEEL CABLE-STAYED BRIDGE BASED ON MONITORING DATA

Yi ZHOU[*], Limin SUN[†], and Shouwang SUN

State Key Laboratory for Disaster Reduction of Civil Engineering, Tongji University, P. R. China

ABSTRACT

In last two decades, structural health monitoring (SHM) technology has been widely and systematically employed for civil engineering structures, especially on long-span bridges around the world. A good SHM system could provide massive amounts of information for structural engineers to facilitate the management and maintenance of complicated structures. It is still a hot research topic that how to make better use of monitoring data among academic researchers and practical engineers.

This paper investigated the temperature field and its effects based on the SHM data of a long-span cable-stayed bridge in Shanghai, China, which has the span arrangement of 92+258+730+258+72 m, completed in 2010. The daily and seasonal temperature variations and thermal induced structural responses, in terms of the deformation of tower and girder, the cable force, and the strain at the mid-span section of girder, were taken into consideration. The monitored data were presented in a summary manner and were further compared with the analytical results of a finite element (FE) model. A good agreement in the variation trend between the field measurements and the analytical results was reached.

The main conclusions of the study include: 1) The structural temperature distribution pattern of the bridge can be explained by the basic heat transfer conditions, i.e. radiation, conduction and convection; the structural temperature is significantly different from the ambient temperature; 2) The thermal-induced structural responses have daily and seasonal cycles. For the daily cycle, the relationship of the response parameters and the girder's average temperature could be modeled by a linear formula. However, the mechanism behind these phenomena deserves a further study; 3) The FE model on the basis of physical meaning could grasp the basic trends of the thermal effects.

The analysis here could provide us invaluable information on the behavior of long-span cable-stayed bridge with a floating girder system; additionally, it would benefit the development of SHM technology in return.

Keywords: Cable-Stayed Bridge, Structural Health Monitoring, Temperature Field, Temperature Effects.

1. INTRODUCTION

Temperature is one of the important environmental factors which have a significant association with many dynamic/static indexes related to structural conditions. It is well known that thermal effects are not only affected by temperature variation itself, but also by structural boundary conditions. Hence, it is far from straightforward to predict the structural responses to thermal variation, especially for a highly statically-indeterminate structure, which has become more and more common in last three decades. Fortunately, the emergence and rapid development of structural health monitoring (SHM) technology make it possible for engineers to understand real structural behaviors in a quantitative manner. Recently, many researchers took advantage of SHM data of long-span bridges

---

to study the relationship between thermal field and structural response, e.g. (Xu et al. 2010; Xia et al. 2013) for Tsing Ma Bridge in Hong Kong, China, (De Battista et al. 2011; Brownjohn et al. 2009) for Tamar Bridge in Scotland, UK, (Cao et al. 2011) for Zhanjiang Bay Bridge in China mainland, to name a few. This paper takes a road-cum-rail bridge as a background project, which is a five-span cable-stayed bridge with dual towers, dual cable planes and separated double-box steel girder, and is a floating system along the bridge's longitudinal axis. In a summary form, this paper presents the temperature distribution pattern and the thermal-induced displacement, deformation and cable force variation, based on the monitoring data in Jan. and Aug., 2012. Furthermore, an FE model was established to verify the observed phenomena. Making effective use of these long-term, on-site and continuously monitored data can provide us valuable information on complicated structures; moreover, it would push forward the development of SHM itself. .

2. TEMPERATURE FIELD

In SHM system of the bridge, the temperature measurement points include the air temperatures inside/outside the girder/tower and the structural temperatures of girder/tower/cable, and all the data channels are sampled at intervals of 1 minute.

2.1. Air Temperature

Figure 1 shows air temperatures recorded by the weather station on the deck of the west girder during two weeks in Jan. and Aug., respectively. It is evident that: 1) whether in winter or in summer, the air temperature inside the steel box girder has much larger variation amplitude than that outside the steel girder; meanwhile, the former lags behind the latter about 2 hours. This phenomenon can be explained by the fact that the air inside the girder exchanges heat with the steel box girder, and heat conduction needs time. 2) The air temperature of girder possesses both diurnal and seasonal changes whereas the air temperature inside the concrete tower only has seasonal variation, which implies the concrete is less able to gain or lose heat from their exterior surfaces.
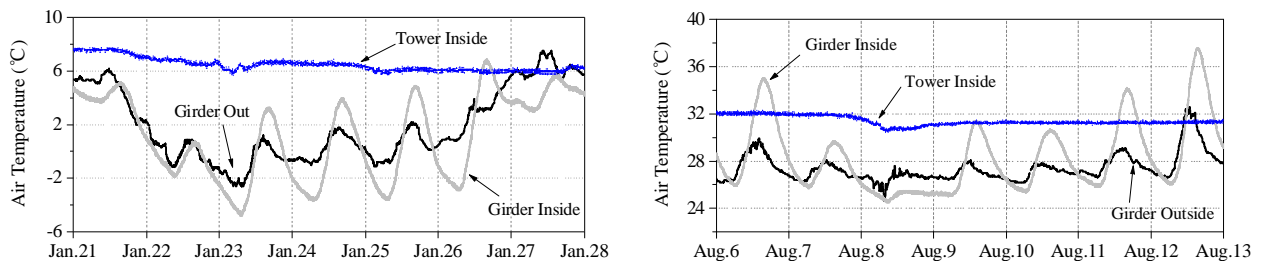

Figure 1: Air temperature comparisons

2.2. Longitudinal Temperature Distribution on Bridge

The temperature on the girder is compared at different sections along the bridge. As shown in Figure 2, 4 time instants are chosen, in which 7:36 and 14:40 are time when the girder's top plate reaches its minimum and maximum temperature on Jan. 23, while 5:44 and 15:12 corresponds to the temperature peak and trough time on Aug. 11. All the temperature values in Figure 2 are the average ones of the two separated box girders. It is worth noting that though the temperature lags among these cross-sections are diminutive, however, the highest temperatures at the two tower-girder intersections are about 5 ℃ lower than the other 3 sections, which might be due to the tower's block of sunshine.
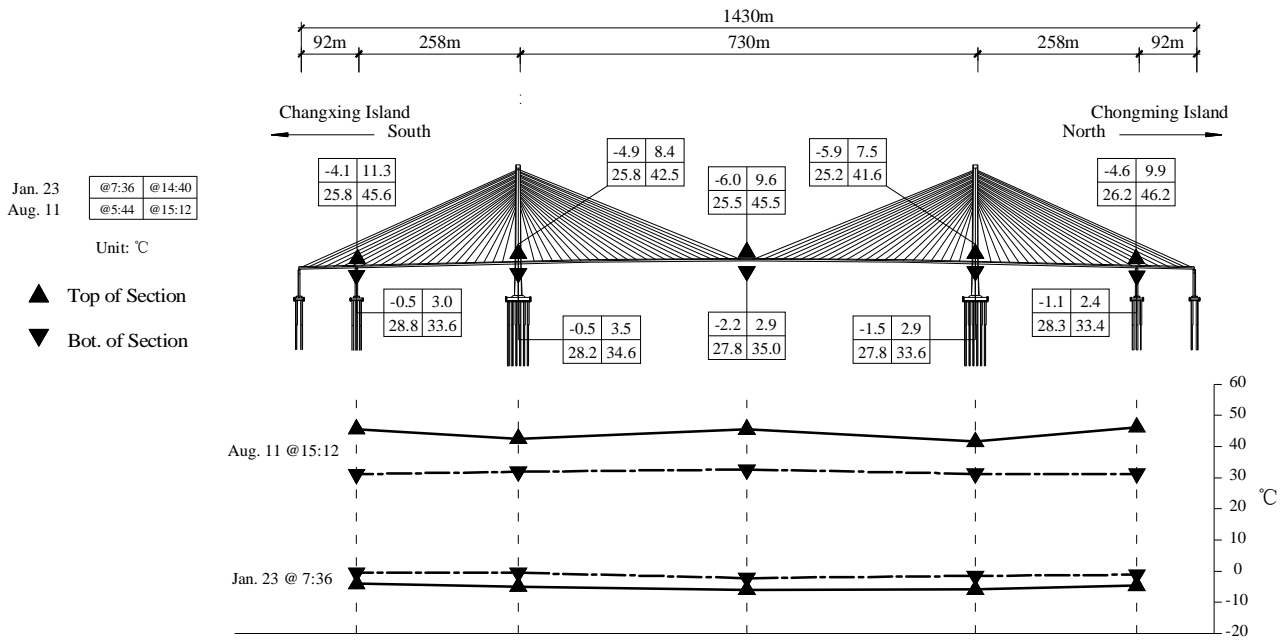
Figure 2: Longitudinal temperature distribution

2.3. Temperature Distribution at Mid-Span of Bridge

Figure 3 is the distribution pattern of structural temperature at the middle section of the bridge's main span. Upon close examination it can be found that: 1) during the high temperature periods, the vertical thermal gradient is much larger than the transverse one, while for the low temperature case, this difference is unclear; 2) steel top plate has a larger thermal variation than bottom plate. Of particular note is that the temperature of these two sensors SST1104 and SST1204 reach their peaks about 3 hours later than the other sensors, which might have something to do with the heat convection condition for the air circulation is weak around their locations.
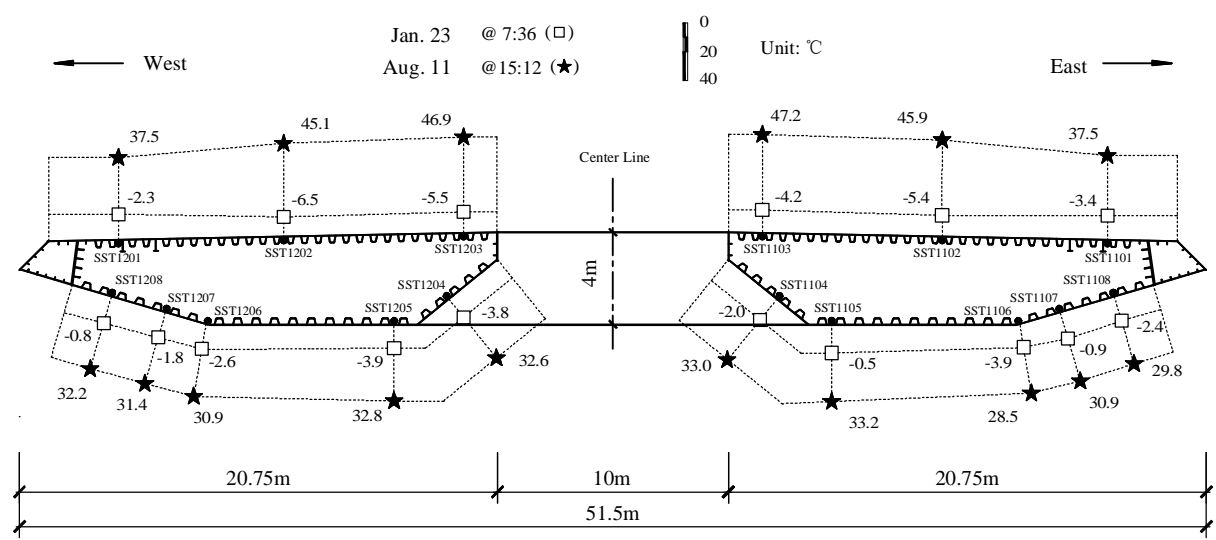

Figure 3: Temperature field at mid-span

2.4. Structural Temperature Comparison

Figure 4 serves the temperature comparison of different structural components and atmosphere. Here, the girder's top plate temperature is the average of SST1102 and SST1202 (Figure 3), and the

3

bottom one is the average of SST1105 and SST1205 (Figure 3); the cable's temperature is the average of the two longest cables SSZ1105 and SSZ1205 (Figure 5) and the tower's temperature is the average of SCT1311 and SCT1314, which locate on the exterior surface facing the south and thus have a larger daily variation than the sensors in the north surface. From Figure 4, the girder's top plate is subjected to the most temperature variation of all, there being a distinct difference in magnitude between the structural temperature and the ambient temperature. So certain modification is required for the temperature range in structural design, which usually comes from the weather database. As a note for the reader, the cable temperature sensor is enclosed in a protective box which also protects the cable force sensor, and is directly attached on the cable's wrapping. As a result, the measured cable temperature is suspected to be different from that of the high-strength steel wires.
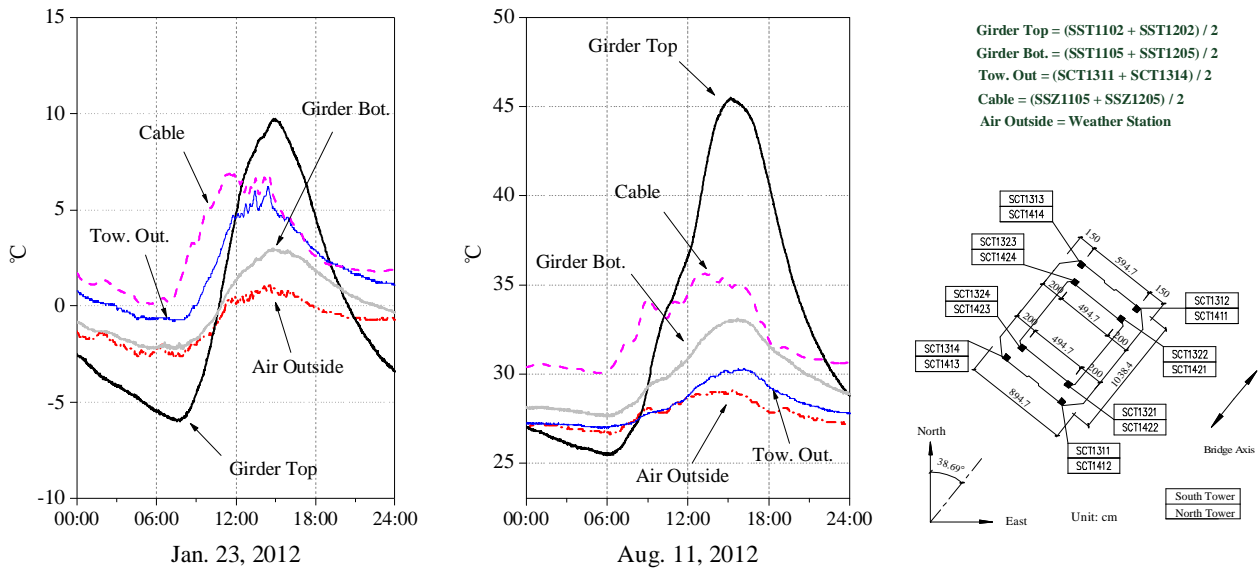

Figure 4: Structural temperature comparison

3.   TEMPERATURE EFFECTS ON BRIDGE

In this paper, the thermal-induced global deformation, local strain and cable force are examined.

3.1. Deformation of Girder

There are totally 4 extensometers installed at the north and south ends of the girder, 2 for each side with a sampling frequency of 20 Hz and the measurements increase if the girder's ends move towards north. In addition, the displacement of the north end minus the south end could approximate the girder's expansion. Figure 5 manifests the strong correlation between girder's longitudinal expansion and the averaged temperature of the girder's top and bottom plates, and the lines of best fit for Jan. and Aug. are also plotted in the figure. The slight difference of the thermal coefficients indicates the existence of somewhat non-linearity seasonally for this cable-stayed bridge.
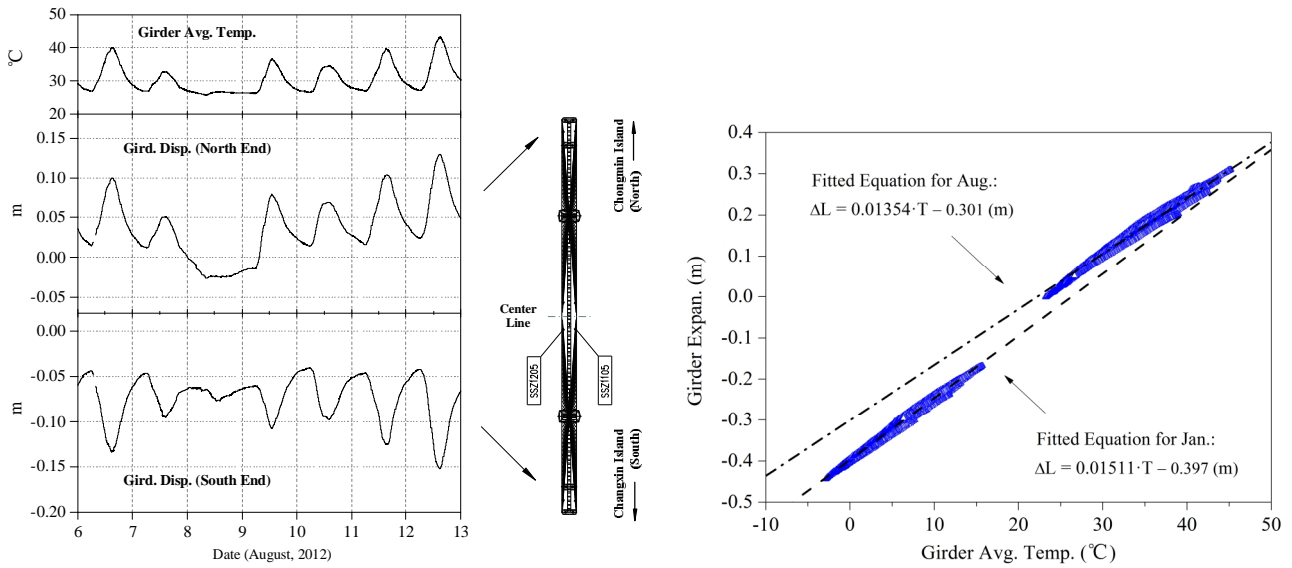
Figure 5: Girder expansion Vs. Girder temperature

GPS technology is used to monitor the girder and tower's displacements at the mid-span and both towers' top with a sampling frequency of 10 Hz. Compared to data from tower, the girder's deflection is seriously affected by the traffic loads. Considering the temperature causes static structural responses, the hourly averages are adopted for GPS data. Figure 6 depicts the relationship between the girder's deflection and its average temperature in August, where an increasing value of the deflection means the girder goes upward. It is obvious that the girder curves upward in the middle with the rise of temperature, and vice verse. This phenomenon is similar to (Cao et al. 2011) but opposite to the observations by (Xu et al. 2010; De Battista et al. 2011), so the mechanism behind this difference remains to be decoded.
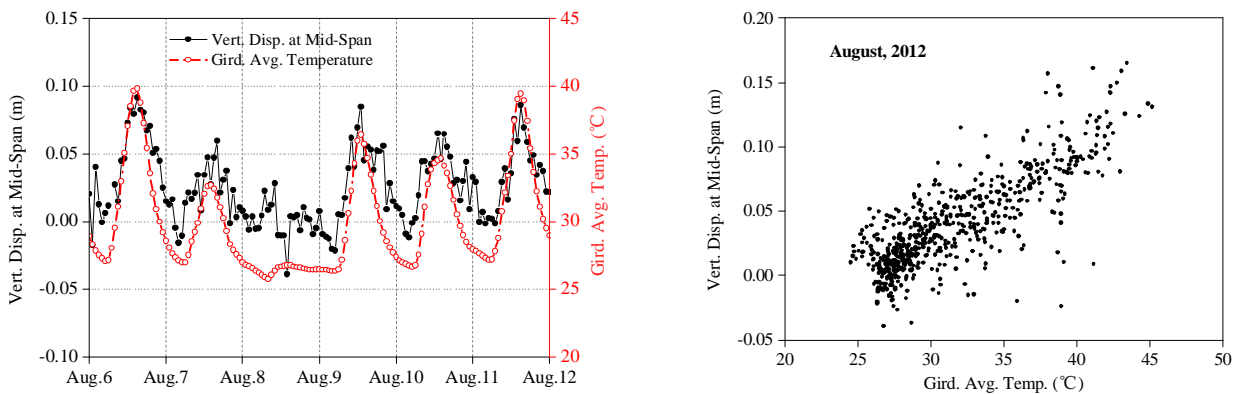

Figure 6: Girder deflection Vs. Girder temperature

3.2. Displacement of Tower Top

The tower's longitudinal displacement is also 1-hour average and the increasing value indicates it moves to the north. From Figure 7 it is interesting to note that the two towers move away from each other when the temperature rises and move close to each other when temperature drops, which follows both the diurnal cycles and the seasonal cycles. Such a result is not so surprising, for it is compatible with the main girder's expansion deformation and elevation changes.
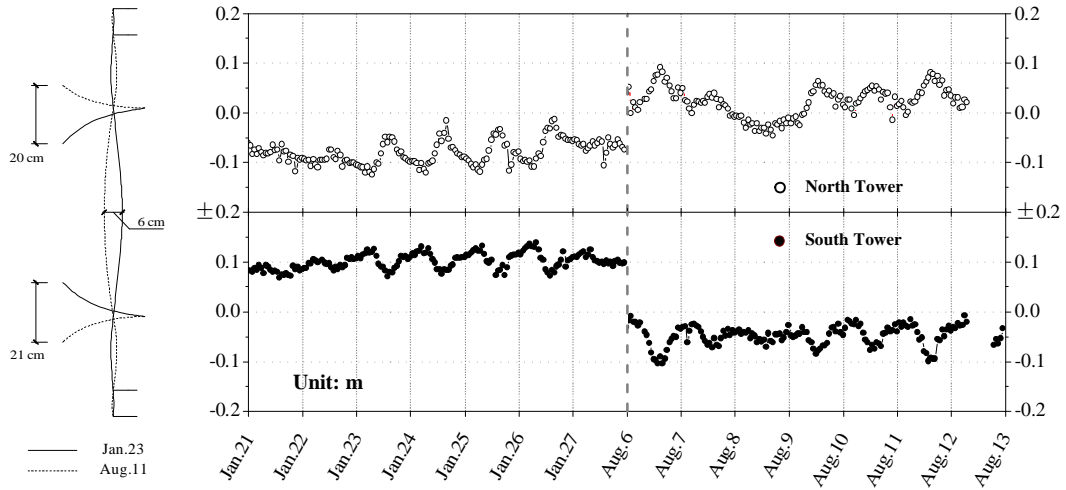
Figure 7: Tower displacement (longitudinal)

3.3. Strain at Middle Section

As a local quantity, strain measurement is collected by FBG sensors with a sampling rate of 20 Hz. In Figure 8 both the measured total strain and elastic strain at the mid-span section are plotted in each subplot, with a positive value representing stretch or tension. Here the measured strain is total strain which contains two parts, i.e. stress-free strain $\alpha \cdot \Delta T$ and elastic strain, the latter being directly related to the stress by the elastic modulus E. Except the temperature, the stain measurements are also affected by random traffic loads significantly; thus 1-min mean value is firstly calculated and then a wavelet packet de-noising algorithm is performed to separate out a smooth thermal-induced strain time history, as represented by the light gray lines in Figure 8. Figure 9 illustrates the relationship between thermal-induced elastic strain and the girder's average temperature based on the August data. The rising temperature will cause an increase of the compressive stress at the top plate; on the contrary, the rising temperature will cause an increase of tensile stress at the bottom plate. A straightforward but not rigorous explanation is that this stress variation pattern comes from the mutual constraints between the upper fibers and lower fibers at the mid-span section in order to keep compatibility condition; after all, the fibers at the top and bottom plates experience much different temperature variation magnitudes.
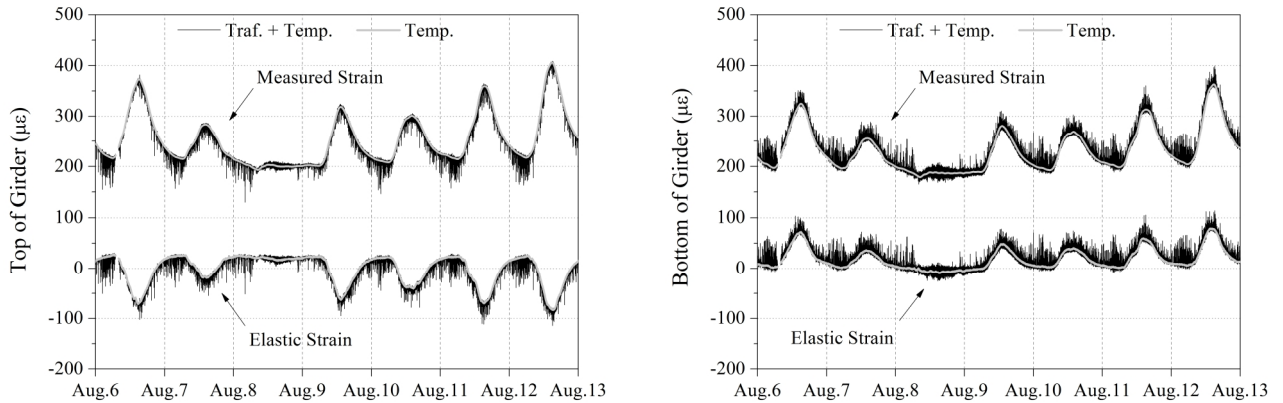

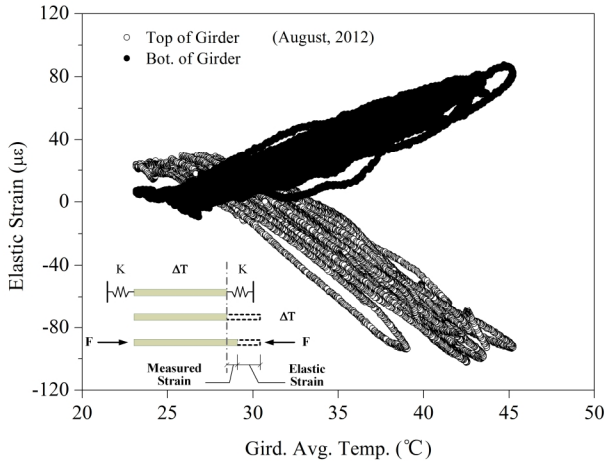**Figure 8: Strain at mid-span of girder**

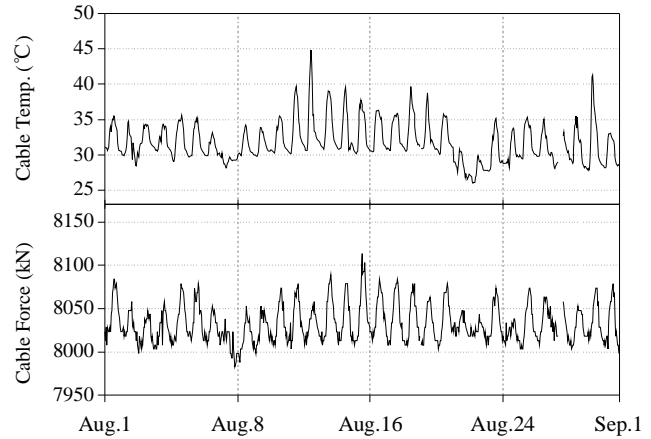**Figure 9: Elastic strain Vs. Girder temp.**   **Figure 10: Cable force and temperature**

3.4. Cable Force

The cable force is estimated from the acceleration signals, which are acquired at a frequency of 50 Hz. For a specific cable, its tension is approximately proportional to the squared natural frequency of some order. Figure 10 shows the time histories in August of the cable SSZ1105's tension and temperature, samples' time interval being 1 hour. The cable force has a positive association with its temperature and the daily variation is rather clear. It should be noted that even though the cable force, boundary conditions and the sag hold constant, the measured frequency of stay-cable would decrease as the temperature increases. According to (Xia et al. 2006) the measured frequency depends more on the elastic modulus E's change than the cable length's variation and the thermal coefficient of E is about -0.036%/℃; on the other hand, cable tension $T \propto f^2 \propto E$ and thus the 20 ℃'s increment of cable temperature in August would cause a decrease of "nominal tension" about 0.72% with all the other conditions unchanged. However, the measured maximum relative change of the cable tension is an increase of 1.48%. Hence, it is inferred that the actual tension change should be more than 1.48%, up to about 2.2% after the temperature modification.

4. FEM RESULTS

By means of FE simulation in the software ANSYS, the measured results are verified qualitatively in terms of the structural response differences among the 4 time instants on Jan. 23 and Aug. 11 mentioned above. The model is a 3D-beam element model with double girders, and the element types Beam44, Beam4, Link10 and Combine14 were used to simulate the main girder, towers, cables and spring boundary conditions, with a total of 1277 elements and 1605 nodes. A good agreement in the variation trend has been observed from Table 1, which confirms the measured results and also indicates the feasibility of the FE model. It is necessary to say, from Table 1 the cable force on Jan. 23 decreases with the rise of temperature, which differs from the situation on Aug. 11. Unfortunately, the corresponding acceleration data in the whole January are not available. Once these data obtained, the comparison would be conducted as soon as possible.

Table 1: Comparison between Measurement and FEM

	$\triangle = Jan23_{High} - Jan23_{Low}$		$\triangle = Aug11_{High} - Aug11_{Low}$		$\triangle = Aug11_{High} - Jan23_{Low}$	
	Measured	Analytical	Measured	Analytical	Measured	Analytical
Gird. Length (m)	0.15	0.17	0.17	0.20	0.67	0.72
Mid-Span Defl.(m)	0.05	0.09	0.08	0.14	0.06	0.13
Tower Dist.(m)	0.11	0.09	0.14	0.11	0.42	0.38
Cable Force Vari. (kN)	-	-30.5	60.1	25.9	-	39.2
Top Total Strain ($\mu\varepsilon$)	114.50	122.24	144.61	149.36	525.69	514.94
Bot. Total Strain ($\mu\varepsilon$)	95.21	122.14	114.62	149.14	470.41	514.20
Top Elas. Strain ($\mu\varepsilon$)	-77.50	-64.96	-94.19	-90.64	-89.91	-103.06
Bot. Elas. Strain ($\mu\varepsilon$)	37.61	60.94	55.82	85.55	66.01	91.80

5. CONCLUSIONS

1) Based on the monitoring data of a long-span cable-stayed bridge, structural temperature distribution pattern could be explained by the basic heat transfer conditions, i.e. radiation, conduction and convection; and the measurements show that the structural temperature is significantly different from the ambient temperature.

2) The thermal-induced structural responses, i.e. deformation and internal force, clearly follow both diurnal and seasonal cycles. For the diurnal cycle, the link between the response quantities discussed here and the average temperature of girder could be modeled by linear formulas, at least for the data in summer. However, the mechanism behind these phenomena deserves a further study. For the seasonal cycle, parts of the structural responses are still not well investigated due to the unavailability of data.

3) The FE model could grasp the basic trends of the thermal effects. Hence, the structural condition could be evaluated based on a fine FE model; at the same time, the FE model could be calibrated according to the field measurements.

The analysis here could provide us valuable information on the behavior of long-span cable stayed bridge with a floating girder system; moreover, it would benefit the development of SHM itself.

REFERENCES

Brownjohn J M W, Worden K, Cross E, et al. (2009). Thermal effects on performance on Tamar Bridge. Proceedings of the 4th International Conference on Structural Health Monitoring of Intelligent Infrastructure (SHMII-4), Zurich, Switzerland.

Cao Y, Yim J, Zhao Y, et al. (2011). Temperature effects on cable stayed bridge using health monitoring system: a case study. Structural Health Monitoring. 10(5), pp. 523-537.

De Battista N, Westgate R, Koo K Y, et al. (2011). Wireless monitoring of the longitudinal displacement of the Tamar Suspension Bridge deck under changing environmental conditions. In Sensors and Smart Structures Technologies for Civil, Mechanical, and Aerospace Systems 2011 (SPIE 2011), Diego, CA, United states.

Xia Y, Chen B, Zhou X, et al. (2013). Monitoring Field monitoring and numerical analysis of Tsing Ma Suspension Bridge temperature behavior. Structural Control and Health Monitoring. 20(4), pp. 560-575.

Xia Y, Hao H, Zanardo G, et al. (2006). Long term vibration monitoring of an RC slab: Temperature and humidity effect. Engineering Structures. 28(3), pp. 441-452.

Xu Y L, Chen B, Ng C L, et al. (2010). Monitoring temperature effect on a long suspension bridge. Structural Control and Health Monitoring. 17(6), pp. 632-653.